Imaging gold clusters on TiO_2(110) at elevated pressures and temperatures

A. Kolmakov and D.W. Goodman *

Department of Chemistry, PO Box 30012, Texas A&M University, College Station, TX 77842-3012, USA
E-mail: goodman@mail.chem.tamu.edu

Received 7 July 2000; accepted 2 October 2000

Variable temperature scanning tunneling microscopy (STM) has been used to image oxide-supported nanoclusters of Au at temperatures from 300 to 450 K and oxygen pressures from 10^{-10} to 4 Torr. Oxygen-induced morphological changes of the $TiO_2(1 \times 2)$ reconstruction are apparent at room temperature and prolonged exposure ($\sim 3 \times 10^3$ L (langmuir)) at 10^{-4} Torr oxygen. Gold clusters with diameters smaller than $\sim$4 nm are unstable toward sintering at ca. 450 K and oxygen pressures $>10^{-1}$ Torr. Oxygen at pressures $>10^{-4}$ Torr weakens the interaction between the gold cluster and the titania support. Increasing the sample temperature to $>$300 K facilitates disruption of the cluster–support interaction.

Keywords: scanning tunneling microscopy, elevated pressures and temperatures, TiO_2, Au clusters, catalysts

1. Introduction

A molecular-level description of gas–surface interactions is a goal of material science, in general, and of heterogeneous catalysis, in particular. Toward this goal single crystal models have been used to simulate more complex technical catalysts. More recently, the "material gap" between technical and single crystal catalysts has been bridged using metal nanoclusters dispersed on ultrathin oxide films [1–4]. The enhanced conductivity of thin oxide films facilitates the utilization of surface analytical methods including scanning tunneling microscopy (STM). These studies have shown that cluster size and the interaction between the cluster and the support strongly influence the activity and selectivity of catalysts [5,6]. The applicability of STM in both ultrahigh vacuum (UHV) and elevated pressures provides a means of bridging the "pressure gap" between the environment typically used with "real world" catalysts and that in surface science studies of model catalysts.

Elevated pressures of reactants are known to profoundly alter the surfaces of catalysts. For example, noble metal clusters below a certain size exhibit morphological changes at reaction conditions as evidenced by *ex situ* STM and XPS [7–9]. In certain instances, reactive Pd metal clusters at elevated temperatures show a marked response to O_2 pressures as low as ca. 10^{-7} Torr [10].

In situ STM studies of metal single crystals at elevated pressures were first used to investigate pressure-induced surface reconstruction at ambient pressures [11]. STM studies of elevated pressures of reactive gas on the morphology of metal clusters and the oxide support have been reported recently [12]. Although these kinds of studies present a formidable challenge, considerable promise lies in STM imaging of oxide-supported nanoclusters at elevated temperatures and pressures. *In situ* imaging is especially relevant to the long-standing problem of deactivation and regeneration of industrial catalysts.

In this letter, we report the first results demonstrating the feasibility of imaging supported nanoclusters with STM at realistic reaction temperatures and pressures. Gold clusters deposited on titania were chosen for this study due to the importance of this system for industrial applications. A critical aspect of this work is demonstrating the ability to target an area of interest while modifying the reactive gas pressure over ten orders of magnitude.

2. Experimental

The experimental setup consists of an UHV analysis/preparation chamber attached to a second chamber housing a commercial (RHK VT-UHV300) variable temperature STM. The analytical chamber contains metal dosers, a single pass cylindrical mirror analyzer (PHI) for Auger electron spectrometer (AES) and an e-beam heater. Both chambers have base pressures of 2×10^{-10} Torr and are separated with a gate valve through which the sample can be transferred. A fast entry-lock is used for sample exchange; *in situ* tip exchange capabilities are also available.

The variable temperature STM utilizes a "walker" scan head mounted on the sample holder with its legs placed on three helical ramps for rapid tip approach and extensive lateral travel. High resolution scans are carried out using a central piezo tube. The chamber also contains facilities for storing and heating samples as well as ion sputtering. While imaging, the UHV-STM chamber can be pressurized to 1000 Torr and the sample heated to 600 K radiantly using a 30 W halogen lamp. The temperature of the sample was

* To whom correspondence should be addressed.

measured with a chromel–alumel thermocouple attached to the edge of the single crystal.

TiO_2(110) crystals (Commercial Crystal Laboratories) were repeatedly sputtered (0.5–2 kV, 0.5–5 μA cm^{-2}, RT) and annealed to ca. 1000 K to produce the (1×1) structure. Reduced samples exhibiting a (1×2) surface reconstruction were obtained by annealing the sample to 1300 K in UHV with the rates of heating and cooling maintained at <3 K s^{-1}. Au clusters were grown via deposition from a thoroughly outgassed and calibrated metal doser with a deposition rate of ca. 10^{-2} ML s^{-1} (ML = monolayer).

Tungsten and Pt/Ir tips were used with the tunneling current maintained between 0.1 and 0.3 nA and a positive sample bias of 1–2 V. Due to the relatively slow damping of the thermal drift, an equilibrium temperature was first established followed by constant current imaging (CCI) of the area of interest. For the elevated pressure experiments, high purity oxygen gas was slowly leaked into the STM chamber while imaging. The STM data were acquired at steady state conditions of pressure and temperature, with the scanning conditions kept constant during the pressure excursion. Since qualitative observations and conclusions are most important here, the cluster size was not corrected for the finite tip radius.

3. Surface morphological changes

In figure 1, the evolution of a 0.3 ML Au deposit on the titania surface is shown as a function of ambient oxygen pressure at 300 K. The initial surface of figure 1(A)

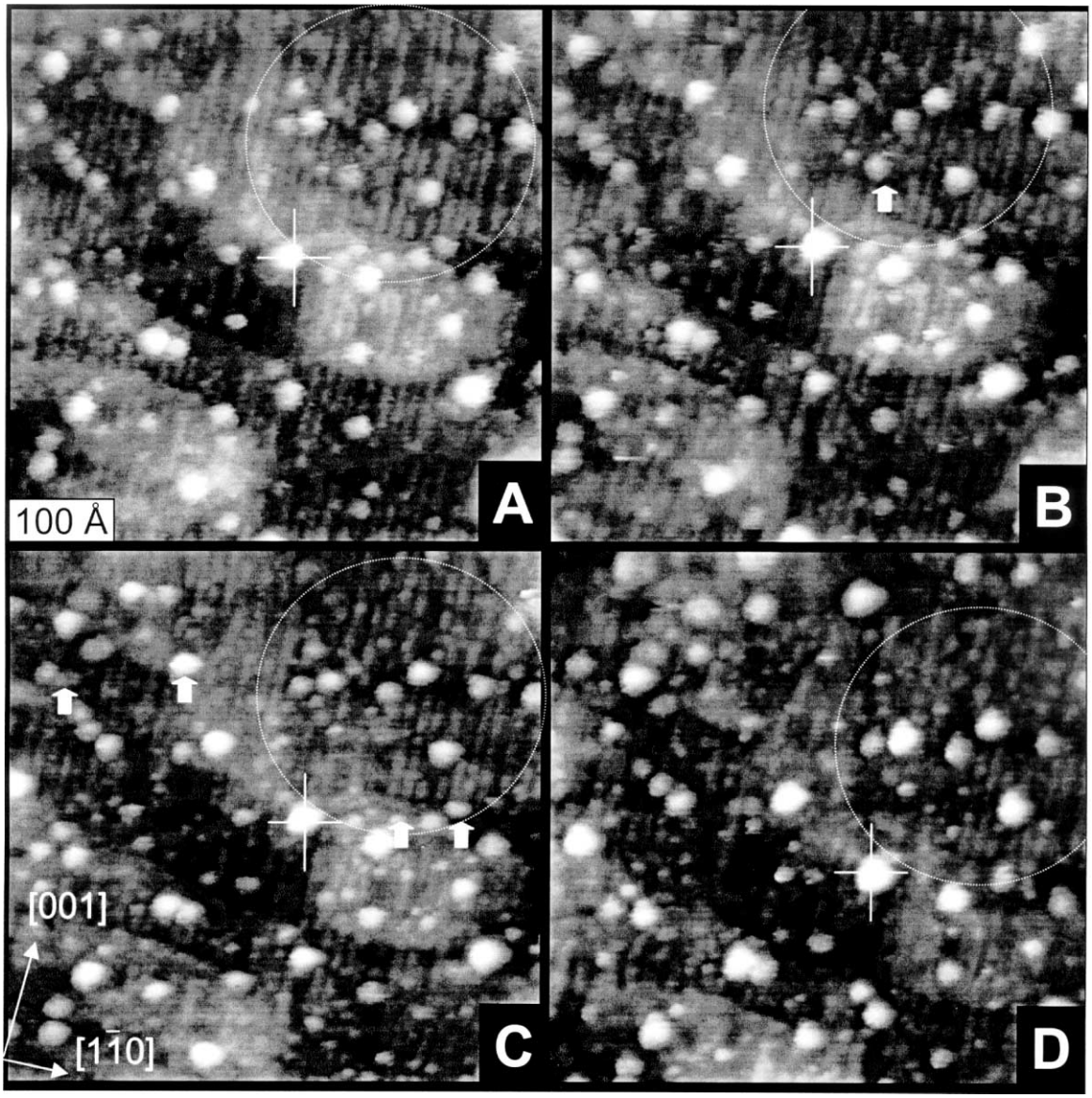

Figure 1. 50×50 nm STM images at 300 K of Au clusters supported on $TiO_2(1 \times 2)$. The central cluster is marked with a cross for reference; moved clusters are marked with arrows. (A) $P_{O_2} = 0$ Torr; (B) $P_{O_2} = 10^{-7}$ Torr, total exposure (TE) 15 L; (C) $P_{O_2} = 1.4 \times 10^{-4}$ Torr, TE $\approx 3 \times 10^3$ L; (D) $P_{O_2} = 10^{-3}$ Torr, TE $\approx 1.2 \times 10^5$ L.

supports Au clusters of 2–5 nm in diameter (0.7 nm average height) on a (1×2) reconstructed $TiO_2(110)$ surface. Several features of this initial surface are noteworthy when exposed to elevated pressures of oxygen:

(i) The (1×2) termination is unstable with respect to elevated oxygen pressures even at room temperature. Disruption and virtual removal of the missing row structure in the marked area (top right corner of figure 1 (A)–(C))

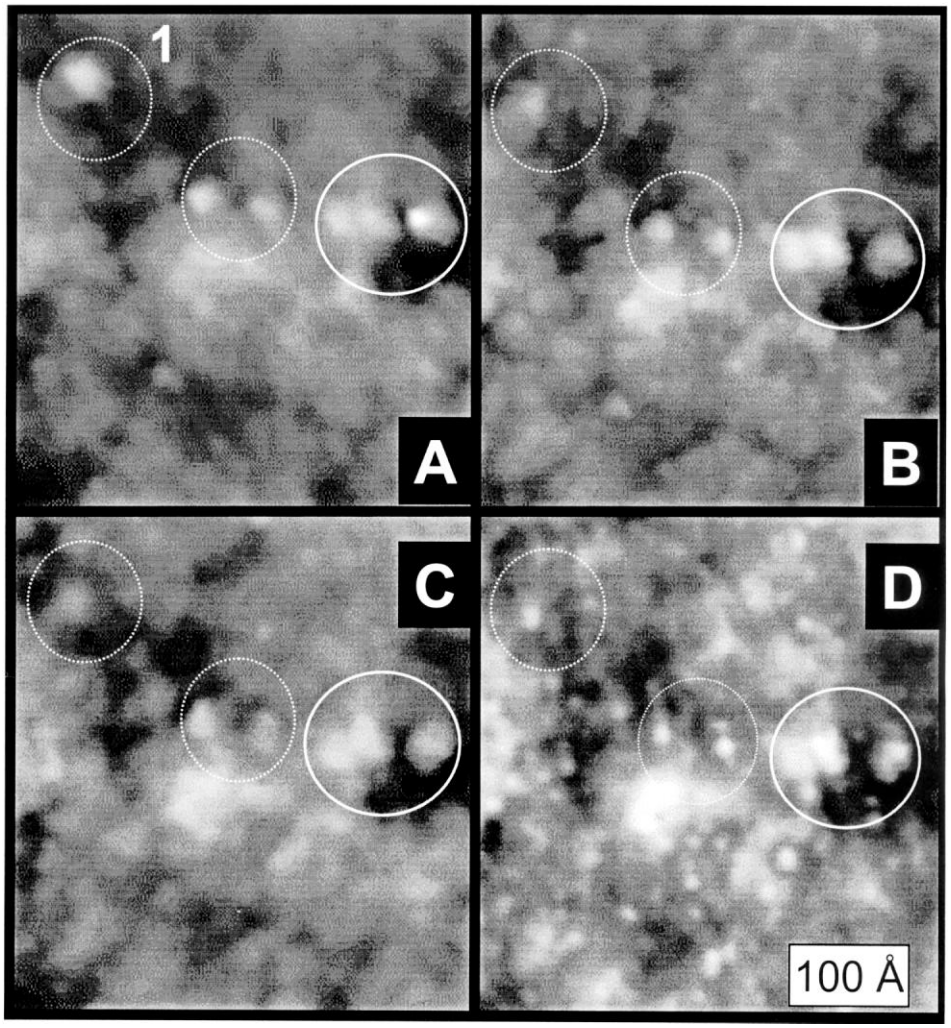

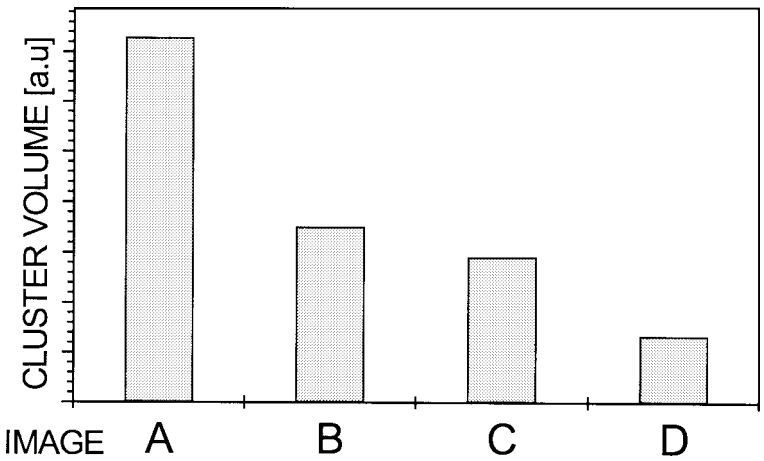

Figure 2. 40×40 nm STM images acquired at 450 K at various oxygen pressures. Gold clusters exhibiting pressure-induced changes are marked with a dashed line; unchanged clusters are marked with a solid line. In the bottom graph the volume of cluster #1 is plotted for the various images. (A) $P_{O_2} = 0$ Torr; (B) $P_{O_2} = 10^{-1}$ Torr, 10 min; (C) $P_{O_2} = 2$ Torr, 90 min; (D) $P_{O_2} = 4$ Torr, 150 min.

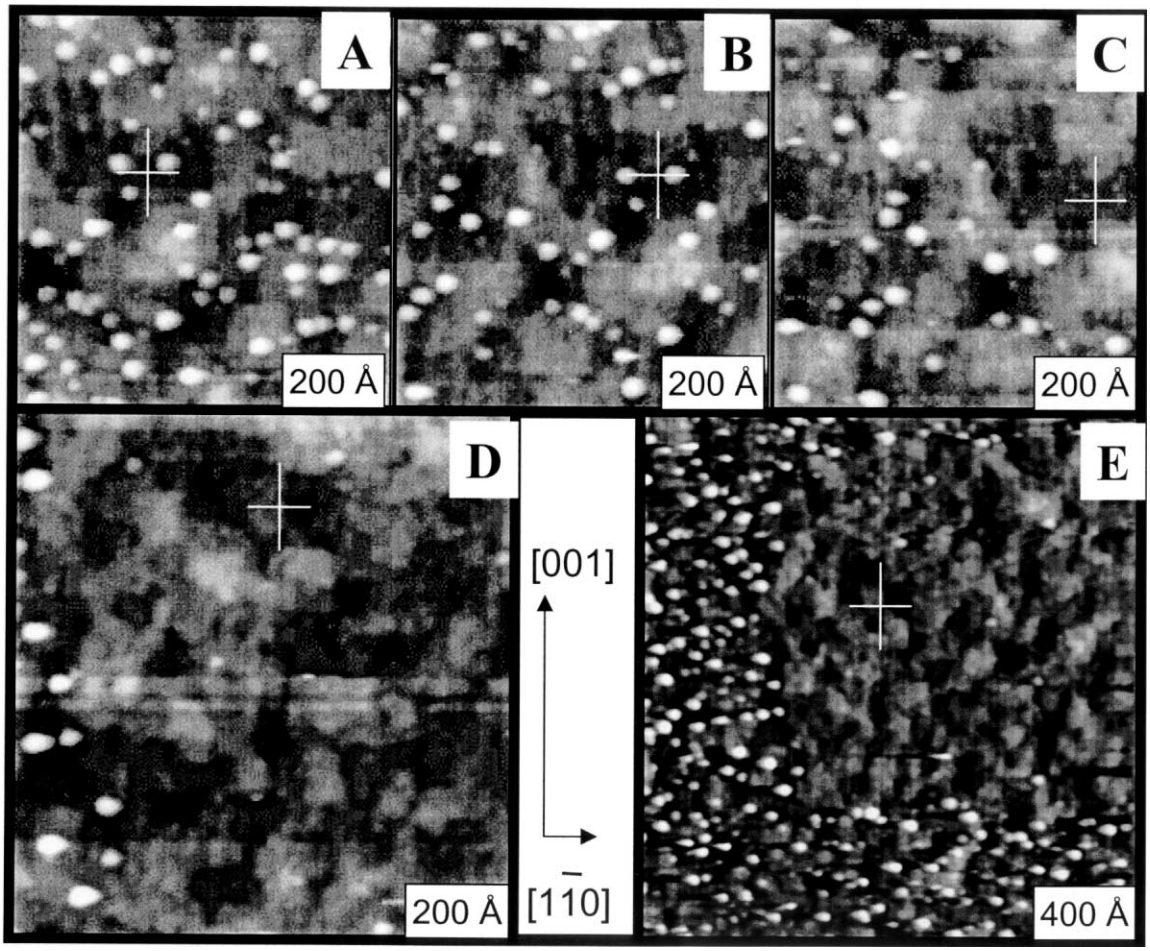

Figure 3. Sequential scans of $TiO_2(1 \times 1)$ surface covered with Au clusters at 430 K. (A) As-prepared 75 × 75 nm. The cross-hairs serve as reference points; (B) $P_{O_2} = 2 \times 10^{-6}$ Torr, 75 × 75 nm; (C) $P_{O_2} = 2 \times 10^{-4}$ Torr, 75 × 75 nm; (D) $P_{O_2} = 2 \times 10^{-4}$ Torr, 100 × 100 nm; (E) $P_{O_2} = 2 \times 10^{-4}$ Torr, 200 × 200 nm.

upon oxygen exposure is evident. In the final image (figure 1(C)) acquired at 10^{-3} Torr, the missing row structure is converted into a net of small clusters and islands oriented along the $\langle 001 \rangle$ direction, presumably having the (1×1) structure. The formation of these small (1×1) islands at elevated temperatures and moderate ($\leqslant$1000 L) oxygen exposures has been reported previously and attributed to the onset of nucleation of a new (1×1) layer promoted by the segregation of interstitial Ti^{+} ions [13,14]. A second explanation is that the newly formed bright protrusions are gold aggregates formed via oxygen-induced Ostwald ripening [8]. Due to the limited resolution of the images it is difficult to choose between these two possibilities; however, the lack of appreciable change in the Au Auger intensity concurrently with the change in the surface morphology suggests the first explanation.

(ii) The Au nanoclusters also undergo pressure/temperature-induced changes. In figure 2, several Au clusters decorating the step edges are imaged as a function of ambient oxygen pressure, although the elevated temperature (∼430 K) limits the resolution. As seen previously for metal single crystals, exposure to oxygen roughens the surface (figure 2(B)). Formation of small protrusions with an average diameter of 1.0 nm is apparent in figure 2(D) upon prolonged exposure. More noteworthy is the continuous disappearance of specific gold clusters (within the dashed circle regions) with increasing oxygen pressure and exposure time. Upon prolonged treatment, the clusters assume a steady state diameter of ca. 1–2 nm. For comparison, two protrusions on the right side of the images appear to be quite stable with respect to this treatment. A similar yet more efficient process of oxygen-induced encapsulation of metal nanoparticles has been recently reported [10] in which Pd becomes buried beneath the TiO_2 substrate via growth of titania about the cluster. This phenomenon originates from surface segregation of interstitial Ti ions and spillover of reactive oxygen from the Pd nanoclusters. A second possibility is disruption of Au–Au bonds upon O_2 treatment of the parent clusters. This possibility has been discussed [7,8] and proposed to account for the observed oxygen-induced sintering of supported gold clusters. This is particularly relevant for Au on TiO_2 since the catalytic properties of Au in

the range of 2–4 nm are significantly different from those of bulk Au.

4. Tip effects and imaging artifacts at elevated pressures/temperatures

Several effects can seriously hamper imaging at elevated pressures and temperatures. In particular, the tip material and condition are crucial. The choice of the tip depends on the reactive gas environment, the sample material and the imaging temperature [15]. In the specific experiments described, etched tungsten tips were used because of their stability in oxygen up to 10^{-4}–10^{-3} Torr; Pt/Ir tips were used to image supported clusters at atmospheric pressure. It is important to avoid unshielded ionization sources (filament, gages and pumps) near ($\leqslant$50 cm) the sample while imaging because of positive ion formation when back filling with gas. The ion current influences the feedback operation of the CCI mode even at 10^{-4} Torr and frequently leads to image loss. Acoustic noise can also be transmitted into the tunneling region at elevated pressures. Back filling the chamber with gas alters the rate of heat dissipation from the sample and induces large thermal drifts beginning at pressures as low as 10^{-4} Torr.

Other complications to imaging include interaction between the tip and the clusters, which is important in STM/STS measurements on weakly bound clusters and biomolecules on oxides [16]. In particular, gold nanoclusters on titania interact very weakly with the support. At certain imaging conditions, tip–cluster interactions may exceed cluster–support interactions resulting in cluster movement or adhesion to the tip. Most probably, this kind of tip modification is responsible for the increase in cluster size evident in figure 1(D). In the series of images of figure 1 (A)–(C), the moved/erased clusters are marked with arrows. In principle, it is possible to eliminate such cluster disturbance by imaging with a large gap resistance of several GΩ. However, although stable to imaging in vacuum, clusters become increasingly mobile at elevated oxygen pressures. In contrast to previous reports of tip-induced cluster mobility [17], the smallest clusters are decidedly more susceptible to being perturbed by the tip. Assuming the cluster–surface interaction is proportional to the number of the gold atoms at the cluster–support interface, these results are consistent with oxygen-induced, gold–substrate bond disruption with the STM tip acting as a promoter. At higher temperatures, the imaged area can be completely modified by this disruption. Figure 3 shows a sequence of images demonstrating this tip-induced cluster mobility. It is noteworthy that a Pt/Ir tip was used in this particular experiment to minimize tip oxidation. As noted in figure 1, the cluster density remains constant at UHV conditions while the clusters gradually disappear with scanning at increased pressure. To rule out tip-induced effects, the imaging area was enlarged (figure 3 (D) and (E)). In the previously unimaged area, the clusters remain intact while those in the scanned have disappeared, presumably “picked up” by the scanning tip.

5. Conclusion

Successful imaging of gold nanoclusters supported on TiO_2 oxide under elevated pressure and temperatures demonstrates the feasibility of using STM for studying model catalysts under realistic reaction conditions. Pressure-related morphological changes were observed for the gold nanoclusters and the titania support with ambient oxygen treatment. Tip quality and tunneling conditions are crucial because of the near coincidence of optimum imaging conditions and tip modifying conditions. For 2–5 nm Au nanoclusters supported on TiO_2, oxygen-induced weakening of the cluster–support interaction at 3–6 GΩ tunneling resistance was observed at a threshold of ca. 10^{-3} Torr; the effect becomes more prominent at elevated temperatures.

Acknowledgement

We acknowledge with pleasure the support of this work by the Department of Energy, Office of Basic Energy Sciences, Division of Chemical Sciences and the Robert A. Welch Foundation. We also thank Dr. C.C. Chusuei for critical reading the manuscript.

References

[1] D.W. Goodman, Chem. Rev. 95 (1995) 523.
[2] C.T. Campbell, Surf. Sci. Rep. 27 (1997) 1.
[3] C.R. Henry, Surf. Sci. Rep. 31 (1998) 235.
[4] M. Baumer and H.-J. Freund, Prog. Surf. Sci. 61 (1999) 127.
[5] M. Valden, X. Lai and D.W. Goodman, Science 281 (1998) 1647.
[6] U. Heiz, F. Vanolli, A. Sanchez and W.-D. Schneider, J. Am. Chem. Soc. 120 (1998) 9668.
[7] M. Valden and D.W. Goodman, Isr. J. Chem. 38 (1998) 285.
[8] X. Lai, T.P. St. Clair and D.W. Goodman, Faraday Discuss. 114 (1999) 279.
[9] H.-P. Steinruk, F. Pesty, L. Zhang and T. Madey, Phys. Rev. B 51 (1995) 2427.
[10] R.A. Bennet, P. Stone and M. Bowker, Faraday Discuss. 114 (1999) 267.
[11] G.A. Somorjai, Appl. Surf. Sci. 121/122 (1997) 1.
[12] A. Berko, G. Menesi and F. Solymosi, J. Phys. Chem. 100 (1996) 17732.
[13] M. Li, W. Hebenstreit, L. Gross, U. Diebold, M.A. Henderson, D.R. Jennison, P.A. Schultz and M.P. Sears, Surf. Sci. 437 (1999) 173.
[14] R.A. Bennet, P. Stone, N.J. Price and M. Bowker, Phys. Rev. Lett. 82 (1999) 3831.
[15] J.A. Jensen, K.B. Rider, Y. Chen, M. Salmeron and G.A. Somorjai, J. Vac. Sci. Technol. B 17 (1999) 1080.
[16] R. Akiyama, T. Matsumoto and T. Kawai, J. Phys. Chem. B 103 (1999) 6103.
[17] P.J. Durtson, R.E. Palmer and J.P. Wilcoxon, Appl. Phys. Lett. 72 (1998) 176.